Fabrication and Characterization of a High-Resolution Neural Probe for Stereoelectroencephalography and Single Neuron Recording

F. Pothof, S. Anees, J. Leupold, L. Bonini, O. Paul, *Member IEEE*, G.A. Orban, P. Ruther, *Member IEEE*

***Abstract*— This paper reports on the design, fabrication, and characterization of neural probes for stereoelectroencephalography (SEEG). The probe specifically targets focal epilepsy as key application. However, probes of this type can also be used for the diagnosis and treatment of other neural dysfunctions such as Parkinson's disease or tremor, typically requiring deep brain probes. The probe fabrication, of which most processes are parallel batch processes, relies on a novel fabrication concept for rolling and gluing thin film polyimide sheets with integrated electrodes into permanent cylindrical shapes with diameters down to 800 µm. The SEEG probes, comprise several macro-electrodes designed to record local field potentials, and micro-electrodes positioned in-between, dedicated to monitoring single unit activity, with a total channel count of 32, despite the small diameter. While platinum micro-electrodes with a diameter of 35 µm have impedances of about 255 kΩ at 1 kHz, impedance values down to about 1.5 kΩ have been measured for the macro-electrodes. The devices have shown good compatibility with magnetic resonance imaging in a 9.4 T magnet, enabling the precise post-operative probe localization within the brain.**

I. INTRODUCTION

Depth probes with multiple electrodes aligned along the probe axis are used in various clinical applications, such as the treatment of Parkinson's disease based on deep brain stimulation (DBS), and the diagnosis of focal epilepsy. In this later case, stereoelectroencephalography (SEEG), introduced by Talairach and Bancaud in the 1950s [1], exploits depth probes to precisely localize the epileptogenic zone via triangulation in patients with drug resistant focal epilepsy in order to surgically resect the involved brain area [2]. Depth probes for these clinical applications most often use platinum-iridium (PtIr) cylinders as electrodes aligned in a pearl chain arrangement with insulating sections between these recording sites. The individual electrodes are connected to an external connector using single wires imposing challenging space constraints in case of a large number of electrodes. Depth probes for DBS typically have a diameter of 1.27 mm and comprise four electrodes. On the other hand, SEEG probes are available with diameters as small as 0.8 mm drastically reducing the impaired brain volume requested in view of up to 15 probes per hemisphere applied in individual patients. These SEEG probes comprise up to 18 electrodes with a length of 2 mm, as demonstrated by Dixi Medical, Besançon, France. Besides the cylindrical macro-contacts of SEEG probes recording local field potentials (LFP), micro-electrodes, using one of the up to 18 possible leads, were integrated by Dixi enabling single unit activity (SUA) to be recorded. This approach has the potential to improve the spatial resolution of triangulation in focal epilepsy diagnosis and to gain a deeper understanding of this dysfunction.

Recent neural probe developments have applied microsystems fabrication processes using polymer layer sandwiches with integrated electrodes. These planar structures have been shaped into probe cylinders by adhesively bonding them to solid carrier pins of appropriate diameters. Examples with 64 individually addressable electrodes have been demonstrated in 1.27-mm-diameter probes [3] and alternative electrode configurations have been described in a patent disclosure [4]. In contrast to these examples, we introduce an approach similar to that used for cuff electrode fabrication [5]. We realized initially hollow cylinders with diameters as small as 800 µm. With 32 channels we present a probe that combines a small impaired brain volume with a high channel count. Further advantages are the inherent encapsulation of the leads and a straightforward assembly process not requiring precision mechanics of the parallel batch processed polyimide (PI) foils.

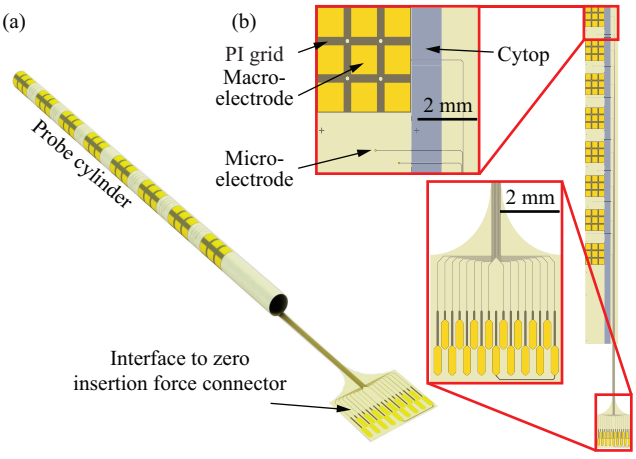

Fig. 1: (a) Schematic of SEEG probe geometry and (b) layout of a flat polyimide layer sandwich foil illustrating macro-contacts and micro-contacts, later brought into cylindrical shape through 3D profiling.

The research leading to these results has received funding from the European Union's Seventh Framework Program (FP7/2007-2013) under grant agreement n°600925.

F. Pothof, S. Anees, O. Paul, and P. Ruther are with the Microsystem Materials Laboratory, Department of Microsystems Engineering (IMTEK), University of Freiburg, Freiburg, Germany (phone +49-761-203-7202, frederick.pothof@imtek.de).

J. Leupold is with the University Medical Center Freiburg, Department of Radiology, Medical Physics, Freiburg, Germany.

G. Orban is with the Department of Neurosciences, Università degli studi di Parma, Parma, Italy.

L. Bonini is with the Istituto Italiano di Tecnologia (IIT), Brain Center for Social and Motor Cognition, Parma, Italy.

978-1-4244-7929-0/14/$26.00 ©2014 IEEE

II. Probe Design

In a first design iteration of the novel SEEG probes schematically shown in Fig. 1(a), the outer diameter was chosen to be similar to that of existing probes for clinical applications. As the probes are initially destined for in vivo recordings with macaque monkeys for validation purposes, the overall probe length was limited to 42 mm. Based on the probe implantation protocol described in Section IV, 32 mm of the total length can be implanted into brain tissue. The probes designed with a diameter of 800 µm comprise in total 16 or 32 channels, i.e., 8 cylindrical macro contacts with a length of 2 mm each, and 8 or 24 micro-electrodes with a diameter of 35 µm. The macro-electrodes comprise a PI grid, as indicated in Fig. 1(b), to protect the underlying platinum (Pt) from scratches or delamination during the 3D profiling process. The macro-electrodes are separated by a distance of 1.5 mm. The 8 or 24 micro-electrodes are positioned around the circumference of the cylinders between the macro-contacts. All electrodes are interfaced to zero insertion force (ZIF) connectors. For the ZIF mating process, a 0.3-mm-thick PCB is introduced in parallel at the backside of the probe ZIF interface to guide the flexible foil into the ridgid connector.

III. Probe Fabrication

The probes are based on a 10-µm-thick PI layer stack comprising a 300-nm-thin Pt metallization for leads and electrodes. To promote long-term adhesion between the PI layers and the metallization sandwiched in-between, the Pt leads are additionally covered by diamond like carbon (DLC) and silicon carbide (SiC) layers [6]. The PI-metal sandwich, as schematically shown in Fig. 1(b), is fabricated on a handle wafer and transferred to the cylindrical probe shape using an annealing step inside a metal mold. The fixation of the probe in its cylindrical shape applies a dry resist that has been applied during the fabrication of the PI layer sandwich. The probe is finally filled with a medical grade epoxy to achieve a probe stiffness appropriate for implantation. The probe fabrication applies a two-stage process: First the PI layer sandwich comprising the electrode metallization is realized; second, by 3D-profiling of this layer sandwich cylinders with a diameter of 800 µm are produced.

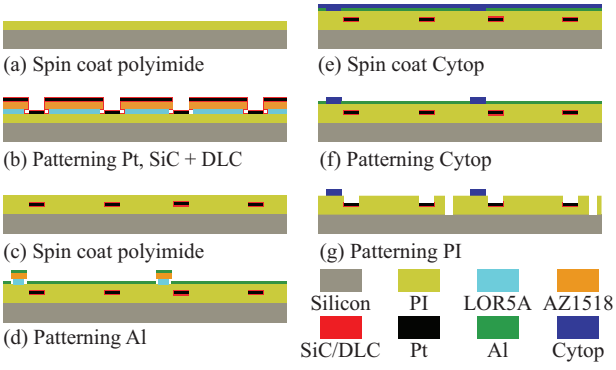

Fig. 2: Probe fabrication based on thin film processing of PI, Pt, Al, SiC, and DLC.

A. Stage 1 - Processing of PI Structure

Fig. 2 details the process sequences of the first stage. It is based on a process technology introduced for the realization of retinal implants [6]. In case of the SEEG probes developed in this study, the process comprises additional steps to deposit and pattern a Cytop® layer, i.e. a fluoropolymer by Asahi Glass Company, Japan, on top of the PI. Similar to PI ribbon cables used for silicon-based probe arrays developed by our group [7][8], PI (U-Varnish S, UBE Industries Ltd., Japan) is spin-coated with a layer thickness of 5 µm onto standard four-inch silicon (Si) wafers {Fig. 2(a)}. In order to facilitate the final removal of the PI layer sandwich from the Si handle wafer, the native silicon oxide layer is removed from the Si using hydrofluoric acid (HF). PI spin-coating and imidization at 450°C is followed by the patterning of SiC (50 nm), Pt (300 nm), SiC (30 nm), and DLC (10 nm) using a lift-off technique based on LOR 5A and AZ 1518 photoresists. Pt and SiC as well as DLC are deposited using sputtering and plasma enhanced chemical vapor deposition (PECVD), respectively {Fig. 2(b)}. Before layer deposition, an oxygen plasma treatment is used to activate the PI surface improving the adhesion of the first SiC film deposited at 100°C. This initial SiC film forms a thin interatomic interface to the PI and thus promotes the long-term adhesion to the PI layer [9]. Then, a second 5-µm-thick PI layer is spin-coated on top of the SiC/Pt/SiC/DLC layer stack {Fig. 2(c)}.

Next, a 100-nm-thick aluminum (Al) layer is deposited and patterned using sputtering and lift-off {Fig. 2(d)}. The Cytop layer serving as a dry adhesive in the subsequent 3D-profiling stage is spin coated on top of the PI sandwich and the Al layer and then soft-baked {Fig. 2(e)}. It is patterned using lithography and reactive ion etching (RIE) {Fig. 2(f)}. The Cytop is removed on top of the Al layer that serves as a hard mask to protect the underlying PI sandwich against the RIE processing. The Al layer is finally removed by wet etching. In a last process sequence, the PI is selectively etched by RIE to open the electrode sites and contact pads, and to define the probe shape {Fig. 2(g)}. This etching step removes possible DLC or SiC residues on the Pt surface as well. The PI layer stack is finally peeled off the wafer using tweezers.

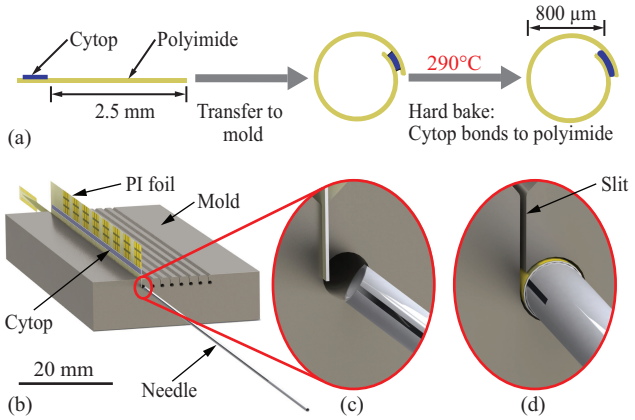

Fig. 3: (a) Schematic of the rolling and bonding processes of polyimide cylinders employing Cytop; (b) Computer model of the mold, (c) close-up of the needle grabing the PI foil, and (d) PI foil rolled-up inside the cavity.

B. Stage 2 - 3D Profiling of PI Sandwich

The 3D profiling of the SEEG probes is achieved through rolling of the PI foils and annealing at elevated temperatures, as schematically shown in Fig. 3(a), using a metallic mold and slitted needle. The mold comprises 42-mm-long hollow cylinders with an inner diameter of 800 µm accessible from the mold top through narrow slits with a width of approximately 80 µm. A model of the mold is shown in Fig. 3(b). The hollow cylinders and slits are realized using electrical discharge machining (EDM) of stainless steel. The PI layer stacks are manually introduced into the mold cylinders through the narrow slits. They are rolled into their cylindrical shape using a slitted needle {Fig. 3(c)} (outer diameter 700 µm; slit realized by EDM) rotated 2.5-times inside the mold cylinder, as indicated in Fig. 3(d). The PI foil and Cytop overlap by 800 µm. Exposing the rolled PI layer stack inside the mold for 4 hours to a temperature of 290°C anneals the PI layer and hard bakes the Cytop film. Due to the excellent adhesion of Cytop to PI, the PI cylinder is fixed to its intended diameter using the Cytop layer as a dry adhesive at the position of the overlapping PI sections. Finally, the probe is filled with a biocompatible epoxy (EPO-TEK® 301-2, Epoxy Technology, Inc., USA) to ensure mechanical stability.

IV. Application Protocol

The SEEG probes {Fig. 4(a)} are designed to be applied in head-fixed macaque monkeys for validation before human use. During their implantation, the probes with lengths of several centimeters need to be guided to the targeted brain area with sub-millimeter precision minimizing their axial misalignment. This guidance will be accomplished by custom-made hollow bone screws to which the probes will be fixed. These screws are similar to those used in clinical applications such as epilepsy diagnosis based on SEEG probes by Dixi Medical. The screws for monkey and human application are compared in Fig. 4(b). In contrast to the screws for human use, screws for monkey skulls are shorter, given the lower thickness of the macaque skull of around 3 mm. We redesigned the screws to be as short as possible, i.e. with an overall length of 8 mm, 3 mm of which protrude from the skull. The protruding section will be mechanically stabilized by dental acrylic. The inner guiding lumen of the bone screw is 6 mm long and has an inner diameter of 840±10 µm. The mismatch between inner screw and outer probe diameters will allow a maximum angular mismatch of 0.54° in probe orientation. With a penetrating probe length of 32 mm this would result in a positional mismatch of 300 µm at the probe tip. Not included in this mismatch calculation is a possible malposition of the screw itself caused by the surgical procedure. The correct probe position in depth is ensured using a titanium (Ti) ring (thickness 1 mm, inner diameter 0.9 mm, outer diameter 2.5 mm) adhesively fixed to the probe using medical grade epoxy resin. The Ti ring itself is fixed to the screw using bone cement. Fig. 4(c) shows a macaque skull replica with a 16-channel probe inserted through a guiding screw. The screw and the protruding ZIF interface are mechanically protected by a chamber witch a cap, shown in blue on Fig. 4(c). Both protective components are designed with the focus on low space consumption in order not to disturb the animals behaviour.

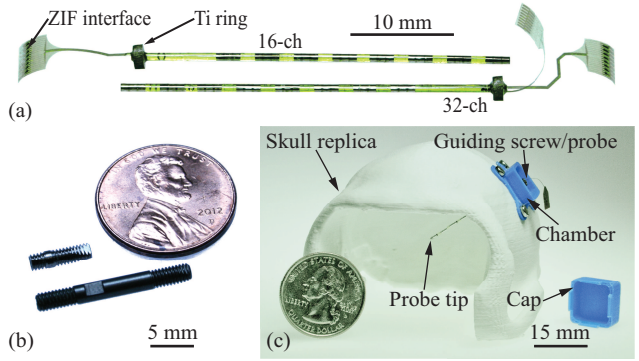

Fig. 4: (a) Assembled 16- (top) and 32-channel probe (bottom) with Ti ring and ZIF interface; (b) Hollow bone screws for probe alignment and fixation; (c) Skull replica with a mounted SEEG probe and protective chamber with cap.

V. Probe Characterization

A. Probe Geometry

The probe geometry was analyzed using a calibrated optical microscope. In a fabrication run with 9 SEEG probes, probe diameters of 794±6 µm were achieved.

B. Electrode Impedance Spectroscopy

The electrode impedance was characterized in 0.9% saline solution using an electrochemical impedance analyzer (CompactStat, Ivium Technologies, The Netherlands), in a 3-electrode setup including a Pt counter electrode, a Ag/AgCl reference electrode, and the electrode of a neural probe

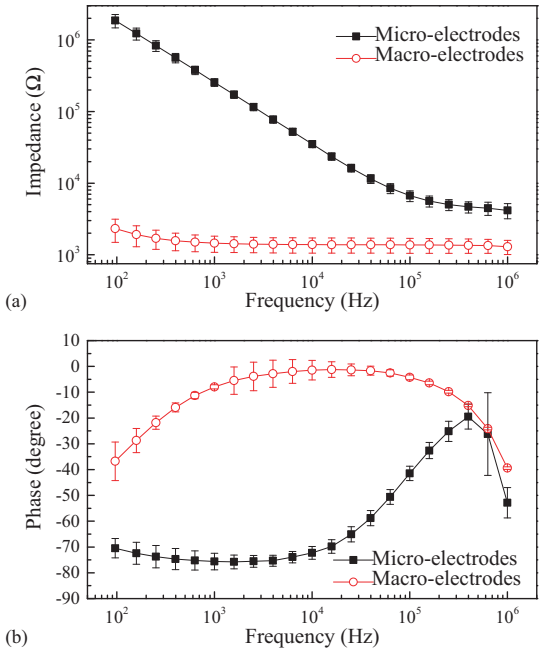

Fig. 5: Frequency dependent (a) absolute value and (b) phase of the impedance of macro- (n = 15) and micro-contacts (n = 27).

applied as working electrode. Figs. 5(a) and (b) show absolute impedance and phase values as a function of frequency for macro- as well as micro-electrodes and their respective standard deviations. The data were averaged over 15 macro- and 27 micro-electrodes of a 32-channel and a 16-channel probe; impedance values at 1 kHz are 1453±369 Ω and 255±31 kΩ for the different electrode sizes, respectively.

C. Magnetic Resonance Imaging

To post-operatively determine the probe positioning in the brain, magnetic resonance imaging (MRI) is useful in particular in view of functional brain imaging. However, MRI tends to be obstructed by image distortion and signal voids caused by the probe geometry and differences in the magnetic susceptibilities of the applied materials. Large artifacts potentially lead to a complete obstruction of magnetic resonance images. On the other hand, small artifacts will hinder the identification of tissue directly in contact with the probe. In order to validate the new SEEG probes and their mounting screw, MR images of the complete setup were taken inside a Bruker Biospec 94/20 9.4 T MRI machine using Gd-doped water as a contrast medium surrounding the sample in a ferrule {Fig. 6(a)}. Imaging was performed with a multi-spin echo sequence (RARE, [10]) with TR = 2 s, TE = 28 ms, and a voxel size $0.16 \times 0.16 \times 1$ mm^3. The representative image in Fig. 6(b) shows only minor artifacts around the probe, which do not interfere with the extraction of the probe position. From the image, the diameter of the probe is determined as 0.9 mm, which corresponds to a field-of-view loss of 0.05 mm on either side of the probe. As expected, the Ti screw causes larger, yet localized, artifacts.

D. Probe Insertion Into Brain Phantom

Insertion tests were performed using a brain phantom made of 0.6% agarose gel that exhibits mechanical characteristics similar to real brain tissue [11]. Neither probe buckling nor probe damage were observed during and after multiple manual insertions of individual probes. Fig. 7(a) shows a probe inserted into the brain phantom. Probe traces were obtained by dipping probes into colored ink prior to their insertion. An example of a trace is shown in Fig. 7(b). Traces indicate a straight insertion path within the phantom.

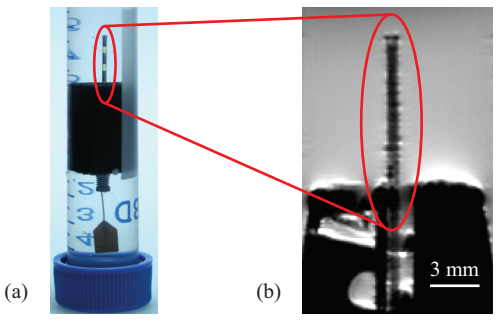

Fig. 6: (a) SEEG probe in a ferrule filled with a contrast medium and (b) MR image taken at 9.4 T.

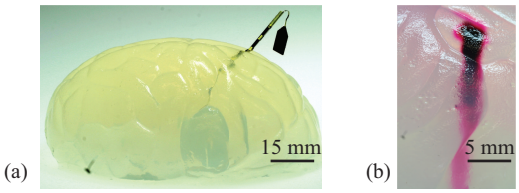

Fig. 7: (a) SEEG probe inserted into brain phatom and (b) traces of ink after insertion.

VI. Conclusion

We have introduced a novel fabrication concept for SEEG neural probes based on a PI layer sandwich. The design and positioning of the electrode sites can easily be adapted to the requirements for individual experiments. To keep the connector space for the test on macaque monkeys as small as possible, we produced 16-channel and 32-channel versions. In the case of human use, we see no obstacle to extending this to 64 or even 128 channels without the need for integrated electronics to time-multiplex the different channels in order to minimize the connector size. With a micro-electrode impedance of 255 kΩ at 1 kHz we expect that it will be possible to record single unit activity from the micro-contacts. Experiments in macaque monkeys will have to confirm our concept regarding measurement quality and biocompatibility. In the future, the electrode material can be changed to iridium oxide in view of electrical stimulation of neural tissue.

Acknowledgment

The authors would like to acknowledge technical discussions and advice in PI process technology by Juan Ordonez, Laboratory for Biomedical Microtechnology at IMTEK, and discussions on the biological application with Leonardo Fogassi and Fausto Caruana, Università degli studi di Parma.

References

[1] J.M. Scarabin, *Stereotaxy and Epilepsy Surgery*. Paris: John Libbey Eurotext, 2012.

[2] A. Palmini et al., "Focal neuronal migration disorders and intractable partial epilepsy: results of surgical treatment," *Annals of Neurology*, vol. 30, no. 6, pp. 750-757, 1991.

[3] E. Toader et al., "Steering deep brain stimulation fields using a high resolution electrode array," in *Engineering in Medicine and Biology Society (EMBC), 2010 Annual Int. Conf. of the IEEE*, Buenos Aires 2010, pp. 2061-2064.

[4] A. Mercanzini and P. Renaud, "Microfabricated neurostimulation device," European Patent Application EP2604313 A1, 2013.

[5] T. Stieglitz et al., "Micromachined, polyimide-based devices for flexible neural interfaces," *J. Biomedical Microdevices*, vol. 2, no. 4, pp. 283-294, 2000.

[6] J.S. Ordonez et al., "A 232-channel retinal vision prosthesis with a miniaturized hermetic package," in *Engineering in Medicine and Biology Society (EMBC), Annual Int. Conf. of the IEEE*, San Diego 2012, pp. 2796- 2799.

[7] S. Kisban et al., "A novel assembly method for silicon-based neural devices," in *World Congr. Med. Phys. and Biomed. Eng.*, 2009, Munich, vol. 25/9, pp. 10710.

[8] P. Ruther et al., "Recent progress in neural probes using silicon MEMS technology," *IEEJ Trans.*, vol. 5, pp. 50515, 2010.

[9] J.S. Ordonez et al., "Long-term adhesion studies of polyimide to inorganic and metallic layers," in *MRS Proc.*, vol. 1466, 2012.

[10] J. Hennig et al., "RARE imaging: A fast imaging method for clinical MR.," *Magn. Reson. Med.*, vol. 3, pp. 823833, 1986.

[11] C. Zhi-Jian et al., "A realistic brain tissue phantom for intraparenchymal infusion studies," *J. Neurosurgery*, vol. 101, pp. 314-322, 2004.